Meccanica (2014) 49:765–773
DOI 10.1007/s11012-014-9908-y

The effect of crack size and specimen size on the relation between the Paris and Wöhler curves

Alberto Carpinteri · Marco Paggi

Received: 31 January 2014 / Accepted: 12 February 2014 / Published online: 1 March 2014

Abstract Paris and Wöhler's fatigue curves are intimately connected by the physics of the process of fatigue crack growth. However, their connections are not obvious due to the appearance of anomalous specimen-size and crack-size effects. In this study, considering the equations for a notched specimen (or for a specimen where failure is the result of the propagation of a main crack) and the assumption of incomplete self-similarity on the specimen size, the relations between the size-scale effects observed in the Paris and Wöhler's diagrams are explained. In the second part of the work, the behaviour of physically short cracks is addressed and, considering a fractal model for fatigue crack growth, the crack-size effects on the Paris and Wöhler's curves are discussed.

Keywords Fatigue · Paris' curve · Wöhler's curve · Incomplete self-similarity · Size-scale effects · Crack-size effects

A. Carpinteri
Department of Structural, Geotechnical and Building Engineering, Politecnico di Torino, Corso Duca degli Abruzzi 24, 10129 Turin, Italy
e-mail: alberto.carpinteri@polito.it

M. Paggi (✉)
IMT Institute for Advanced Studies Lucca, Piazza San Francesco 19, 55100 Lucca, Italy
e-mail: marco.paggi@imtlucca.it

List of symbols

a	crack length [L]
a_{in}	initial crack length [L]
a_0	El Haddad characteristic short-crack length [L]
C	coefficient of the Paris' law [physical dimensions dependent on m, see Eq. (1a)]
d	grain size [L]
$\mathrm{d}a/\mathrm{d}N$	crack growth rate [L]
E	elastic modulus [FL^{-2}]
h	specimen size [L]
m	Paris' power-law exponent
n	Wöhler's power-law exponent
N	number of cycles [−]
N_{cr}	minimum number of cycles for the validity of the Wöhler's regime [−]
N_{th}	maximum number of cycles for the validity of the Wöhler's regime [−]
R	loading ratio [−]
v_{cr}	critical crack growth rate for unstable crack growth [L]
v_{th}	crack growth rate for infinite life (threshold value) [L]

Greek symbols

ΔK	stress-intensity factor range [$\mathrm{FL}^{-3/2}$]
ΔK_{th}	fatigue threshold [$\mathrm{FL}^{-3/2}$]
$\Delta\sigma$	stress range [FL^{-2}]
$\Delta\sigma_{fl}$	fatigue limit [FL^{-2}]
K_{IC}	fracture toughness [$\mathrm{FL}^{-3/2}$]
σ_y	yield strength [FL^{-2}]
σ_0	coefficient of the Wöhler's power-law [FL^{-2}]

1 Introduction

The problem of specimen-size and crack-size effects on fatigue crack growth is of paramount importance in engineering applications. In aeronautical engineering, for instance, the engine failure and the wing cracks observed on a Quantas AIRBUS A380 Aircraft in Singapore in 2010 were attributed to fatigue and required extraordinary maintenance and inspections. The European Air Safety Agency confirmed that the widespread of A380 defects could pose a safety risk in the world's biggest passenger aircraft if left unremedied. The EU agency recommended in its directive to airlines that this kind of failure, if not detected and corrected, may lead to a reduction in structural integrity of airplanes. Fatigue crack growth is also very important for the lifetime of railway axles subjected to impacts of cyclic nature. These components, designed for at least 30 years of service, are one of the most important elements of railway systems and a completely fail-safe design is not yet available.

In all of these cases, the ability to predict the fatigue life with analytical or computational methods is not satisfactory today. Lazzeri and Salvetti [1] proposed a comparison among the existing fatigue life predictions obtained from the application of design softwares based on the original Paris' law [2–4] and its subsequent improvements. The difference between tests and predictions was quite remarkable, as shown in Fig. 1a where the crack length is plotted versus the flight hours, proportional to the number of pressurization/depressurization cycles experienced by airplanes. Twelve years later, similar large deviations between computations and experiments have been noticed by Jones et al. [5] in the short-crack regime, see Fig. 1b, pointing out the problem of reliability of modelling predictions is still open.

The large errors of the existing design methods, crucial for structural integrity assessment, are due to a range of factors. One of the most prominent regards the fact that the existing design formulae have mostly been tuned on fatigue tests carried out at the laboratory scale, although size-scale effects were already noticed by Weibull in 1951 [6]. This was also motivated by the well-known Paris' law [2–4], which says that the crack growth rate of geometrically similar specimens of different size is the same, provided that the stress-intensity factor range at the crack tip is unchanged. The experimental evidence, however, does not confirm this self-similar behaviour and full-sized structural elements present deviations from the Paris' regime.

This anomalous behaviour has recently been highlighted in a special issue on damage tolerance of railway axles edited by Beretta and Zerbst [7], where the fatigue response of full-scale axles has been compared with that of down-scaled specimens. Luke et al. [8] determined the Paris' curves of 1:3 down-scaled specimens and of full-scale axles [M(T)], see Fig. 2. For a given stress-intensity factor range, full-scale components (grey dots in Fig. 2) have a faster crack growth rate than down-scaled samples (coloured triangles in Fig. 2, please refer to the online version for colours).

In the same special issue, size-scale effects have been noticed in the Wöhler's diagram by Makino et al. [9], see Fig. 3. The comparison between the Wöhler's curves obtained from testing down-scaled (40 and 150 mm of diameter) and full-scale (209 mm of diameter) axles shows that the larger the specimen,

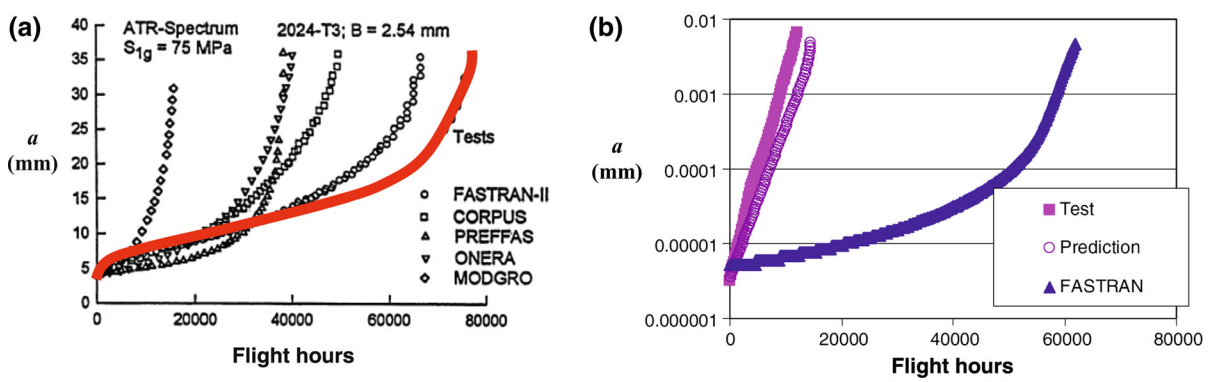

Fig. 1 Predicted and real crack length a versus flight hours. **a** Comparison in [1], **b** comparison in [5]

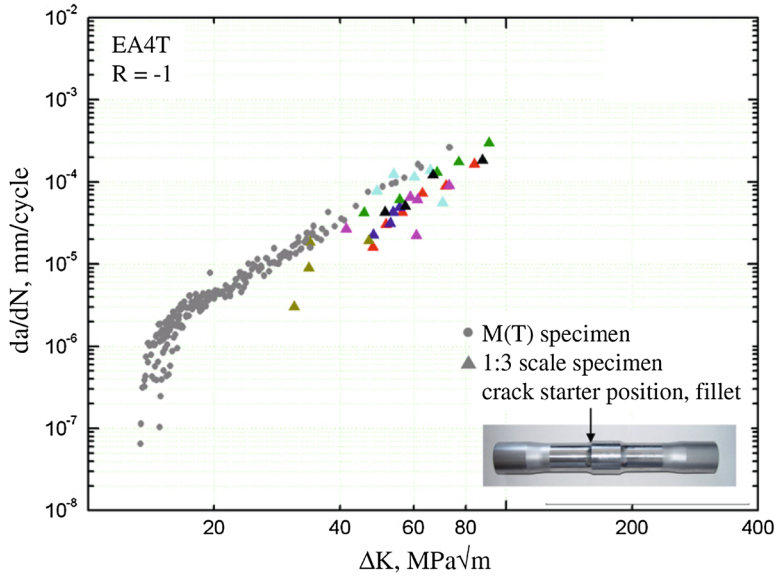

Fig. 2 Size-scale effects on the Paris' curve (adapted from [8])

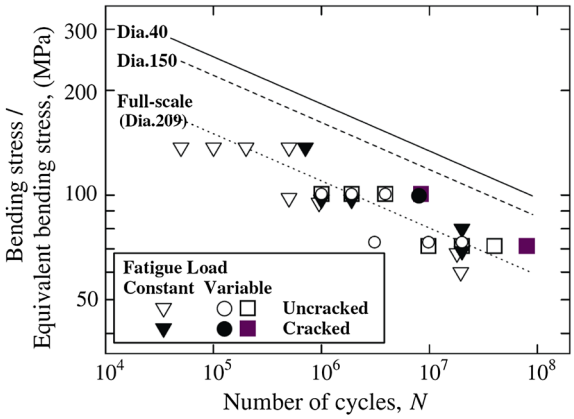

Fig. 3 Size-scale effects on the Wöhler's curve (adapted from [9])

the fewer the cycles to failure, for a given applied stress range.

At present, to the best of the authors' knowledge, no theoretical model is able to consistently interpret these size-scale effects in a unified way. A preliminary effort towards modelling size-scale effects on the Paris' curve has been made by Barenblatt and Botvina [10] (see also [11]). They pointed out that size-scale effects constitute a breakdown of physical similitude and self-similarity in fatigue and found that the Paris' law exponent is specimen-size dependent. This problem was subsequently re-examined by Ritchie [12] and by Ciavarella et al. [13], who considered more experimental data to support these conclusions. A further step towards the understanding of this problem was made in [14, 15], where it was concluded that incomplete self-similarity implies size-scale effects on the second parameter of the Paris' law as well. Always in [14], similar strategies based on dimensional analysis were applied to the Wöhler's curve, which was also theoretically found to be dependent on the specimen size. However, due to a lack of experimental data, this scaling arising from theoretical arguments was not completely confirmed.

In this article, the influence of specimen-size and crack-size effects on the relations existing between Paris' and Wöhler's curves is examined. In case of notched specimens, a set of eight equations in eight unknowns, the coordinates of the points in the Paris' and Wöhler's planes defining the range of validity of the corresponding power-law regimes, is established. The manipulation of the various equations clarifies the connection between the coefficients entering the Paris' and Wöhler's representations of fatigue. As a main conclusion in Sect. 2, it is shown that the equation set based on classical Linear Elastic Fracture Mechanics (LEFM) formulae partially predict size-scale effects which are however not confirmed by the experimental evidence. In order to resolve these inconsistencies, the assumption of incomplete self-similarity is put forward in Sect. 3, to complement the equation set derived in Sect. 2. As a result, the refined formulation is able to capture the experimental trends and provides the first theoretical formulation able to interpret the

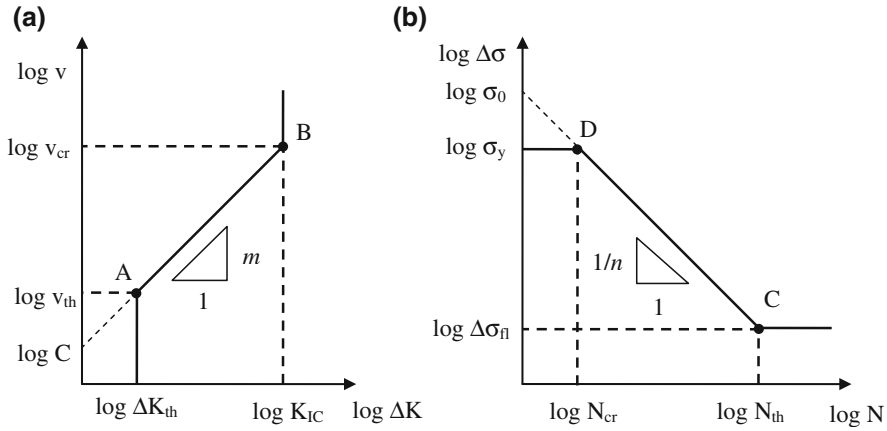

Fig. 4 Paris' curve (**a**) and Wöhler's curve (**b**)

size-scale effects on the Paris' and Wöhler's curves at the same time.

In Sect. 5, the problem of short cracks is considered according to the formulation proposed by the present authors in [16]. By integrating the generalized crack growth law, the deviation from the Paris' law is observed in the Paris' plot near the fatigue threshold. In the Wöhler's diagram, on the other hand, an effect on the slope is noticed depending on the point of transition from the short to the long crack regimes.

2 Expected size-scale effects on the Paris and Wöhler curves of notched specimens according to classical LEFM equations

The curves by Paris and Wöhler are schematically shown in Fig. 4. In these bi-logarithmic diagrams, the crack growth rate, $v = \mathrm{d}a/\mathrm{d}N$, or the cycles to failure, N, can be determined as functions of a loading parameter, ΔK or $\Delta\sigma$. Within a range of the loading parameter, $\Delta K_{th} < \Delta K < K_{IC}$ or $\Delta\sigma_{fl} < \Delta\sigma < \sigma_y$, experimental results can be well interpreted in terms of power-law (straight line in the bi-logarithmic representation), i.e., the Paris' law [2–4], see Eq. (1a), and the Wöhler's law [17], see Eq. (1b):

$$v = C\Delta K^m \tag{1a}$$

$$N = (\sigma_0/\Delta\sigma)^n \tag{1b}$$

The coefficients C and σ_0, as well as the exponents m and n, have been for a long time treated as material constants. Nowadays, their dependency on the structural size and on the initial defect size are established facts at the research level [5, 13] and an effort is made to better quantify these effects for the proposal of new standardized testing methods accounting for them.

Special attention is now given to the coordinates of the points defining the limit of validity of the power-law relations (1a) and (1b). The y-coordinates of the points A and B in Fig. 4a can be related to the x-coordinates of the points C and D in Fig. 4b through the characteristic specimen size h:

$$N_{th} = h/v_{th} \tag{2a}$$

$$N_{cr} = h/v_{cr} \tag{2b}$$

In other words, assuming the simplified hypothesis that cracks propagate with a constant velocity, the number of cycles to failure can be computed as the ratio between the specimen size, h, and the crack velocity, v. The x-coordinates of the points A and B in Fig. 4a can also be related to the y-coordinates of the points C and D in Fig. 4b through the initial defect size, a_{in}. In the case of a Griffith crack, for instance, LEFM provides:

$$\Delta K_{th} = \Delta\sigma_{fl}\sqrt{\pi a_{in}} \tag{3a}$$

$$K_{IC} = \sigma_y\sqrt{\pi a_{in}} \tag{3b}$$

Eqs. (2) and (3) constitute a set of four equations in eight unknowns, i.e., the coordinates of the points A, B, C and D (ΔK_{th}, v_{th}, K_{IC}, v_{cr}, $\Delta\sigma_{fl}$, N_{th}, σ_y, N_{cr}), provided that a_{in} and h are given. Four additional equations can be considered by noting that points A and B belong to the Paris' curve and points C and D belong to the Wöhler's curve. This is also equivalent to writing the coefficients C and σ_0 and the exponents m and n as functions of the coordinates of the points A, B, C and D. In formulae, using Eqs. (1a) and (1b), we obtain:

$$v_{\text{th}} = C\Delta K_{\text{th}}^{m} \tag{4a}$$

$$v_{\text{cr}} = C\Delta K_{\text{IC}}^{m} \tag{4b}$$

$$N_{\text{cr}} = \left(\sigma_0/\sigma_{\text{y}}\right)^{n} \tag{4c}$$

$$N_{\text{th}} = \left(\sigma_0/\Delta\sigma_{\text{fl}}\right)^{n} \tag{4d}$$

Eqs. (2)–(4) constitute a nonlinear set of eight equations in eight unknowns. If the eight conditions were independent, then the ambitious problem to relate the coordinates of the points A, B, C and D to the specimen size h and to the initial defect size a_{in} could be solved. At this stage of the analysis, without any limitation, the parameters C, σ_0, m and n might be constants or given functions of h and a_{in}.

The nonlinear equation set can be solved by progressively eliminating the variables with a series of substitutions. For instance, Eqs. (2a) and (2b) permit to eliminate N_{th} and N_{cr} from the variables. Introducing Eqs. (2a) and (2b) into Eqs. (4c) and (4d), the set of equations becomes:

$$\Delta K_{\text{th}} = \Delta\sigma_{\text{fl}}\sqrt{\pi a_{\text{in}}} \tag{5a}$$

$$K_{\text{IC}} = \sigma_{\text{y}}\sqrt{\pi a_{\text{in}}} \tag{5b}$$

$$v_{\text{th}} = C\Delta K_{\text{th}}^{m} \tag{5c}$$

$$v_{\text{cr}} = C\Delta K_{\text{IC}}^{m} \tag{5d}$$

$$h/v_{\text{cr}} = \left(\sigma_0/\sigma_{\text{y}}\right)^{n} \tag{5e}$$

$$h/v_{\text{th}} = \left(\sigma_0/\Delta\sigma_{\text{fl}}\right)^{n} \tag{5f}$$

Similarly, Eqs. (5c) and (5d) can be used to eliminate v_{th} and v_{cr} from Eqs. (5e) and (5f):

$$\Delta K_{\text{th}} = \Delta\sigma_{\text{fl}}\sqrt{\pi a_{\text{in}}} \tag{6a}$$

$$K_{\text{IC}} = \sigma_{\text{y}}\sqrt{\pi a_{\text{in}}} \tag{6b}$$

$$h/\left(C\Delta K_{\text{IC}}^{m}\right) = \left(\sigma_0/\sigma_{\text{y}}\right)^{n} \tag{6c}$$

$$h/\left(C\Delta K_{\text{th}}^{m}\right) = \left(\sigma_0/\Delta\sigma_{\text{fl}}\right)^{n} \tag{6d}$$

Finally, introducing Eqs. (6a) and (6b) into the remaining two equations, we find, after some manipulation:

$$\begin{aligned}\sigma_{\text{y}}^{n} &= \sigma_{\text{y}}^{m}\sigma_0^{n}C(\pi a_{\text{in}})^{m/2}/h, \text{ or } \sigma_{\text{y}} \\ &= \sqrt{[n-m]\sigma_0^{n}C(\pi a_{\text{in}})^{m/2}/h}\end{aligned} \tag{7a}$$

$$\begin{aligned}\Delta\sigma_{\text{fl}}^{n} &= \Delta\sigma_{\text{fl}}^{m}\sigma_0^{n}C(\pi a_{\text{in}})^{m/2}/h, \text{ or } \Delta\sigma_{\text{fl}} \\ &= \sqrt{[n-m]\sigma_0^{n}C(\pi a_{\text{in}})^{m/2}/h}\end{aligned} \tag{7b}$$

Here, we note that, if m is different from n, the result leads to the paradoxical solution $\sigma_{\text{y}} = \Delta\sigma_{\text{fl}}$, that is against the initial hypothesis of $\sigma_{\text{y}} > \Delta\sigma_{\text{fl}}$, see Fig. 4b. However, if we compute the ratio of Eq. (7a) to Eq. (7b), we obtain:

$$\left(\sigma_{\text{y}}/\Delta\sigma_{\text{fl}}\right)^{n} = \left(\sigma_{\text{y}}/\Delta\sigma_{\text{fl}}\right)^{m} \tag{8}$$

and this equality can be satisfied if and only if $n = m$. It is very interesting that this result is usually obtained following a totally different route, that is, by obtaining the Wöhler's law from the integration of the Paris' equation [14]. Considering the Mode I stress-intensity factor for a Griffith crack of a generic crack length a, $\Delta K = \Delta\sigma\sqrt{\pi a}$, the integration of Eq. (1a) from an initial crack length, a_{in}, to the final one, a_{fin}, gives ($m > 2$):

$$N = \left[C(m/2-1)\pi^{m/2}\right]\Delta\sigma^{-m}a_{\text{in}}^{(1-m/2)} \tag{9}$$

that matches Eq. (1b) if $m = n$. This proves the ability of the initial set of equations to describe the phenomenon of fatigue, interpreted by using either the Paris' or the Wöhler's approach. Introducing $n = m$ into Eq. (7a) or (7b), we obtain an additional condition for σ_0:

$$1 = \sigma_0^{m}C(\pi a_{\text{in}})^{m/2}/h \;\Rightarrow\; \sigma_0 = (\pi a_{\text{in}})^{-1/2}(h/C)^{1/m} \tag{10}$$

Introducing this expression for σ_0, as well as the condition $n = m$ into Eqs. (6c) and (6d), after simplification of the resulting equations we find that they coincide with Eqs. (6a) and (6b). Hence, we conclude that the original eight equations are not independent. Physically speaking, as demonstrated above, the initial equation set implies that the parameters σ_0 and n of the Wöhler's curve are intimately related to the parameters of the Paris' curve and are not independent parameters. We can therefore conclude that the determination of the position of the points A, B, C and D as a function of the initial defect size and of the specimen size is not possible solely with the aid of the eight equations above. This conclusion is general and holds not only when C and m are constant, but also if they depend on h and a_{in}.

To determine how the position of the points A, B, C and D changes by varying h and a_{in}, we need to fix two of the eight unknowns of the problem. A possibility is to select two coordinates of the points A and B of the Paris' curve, e.g., the material fracture toughness, K_{IC}, and the conventional value of crack growth rate for

infinite life, $v_{th} = 10^{-9}$m/cycle. The remaining unknown coordinates of the points A and B, v_{cr} and ΔK_{th}, can be obtained from Eqs. (5d) and (5c), respectively. Hence, if C and m are independent of the initial crack size and of the specimen size, as in the case of complete self-similarity in the respective dimensionless numbers, see the discussion in the next section, then it turns out that the coordinates of the points A and B are also independent of h and a_{in}. Thus, the Paris' curve would be size-scale independent.

Examining the Wöhler's power-law, the y-coordinates of the points C and D can be obtained from Eqs. (6a) and (6b) and therefore they do depend on a_{in}. Finally, N_{th} and N_{cr} can be computed from Eqs. (2a) and (2b) and hence they are dependent on the specimen size.

3 The hypothesis of incomplete self-similarity to interpret the actual experimental trends

Following the pioneering work by Barenblatt and Botvina [10], the assumption of incomplete self-similarity has been put forward by the present authors to explain the size-scale [14], the crack-size [16, 18], and the grain-size [19] effects on the Paris' curve. Recalling the fundamental results established in those articles, the fatigue response represented by the crack growth rate, $v = \mathrm{d}a/\mathrm{d}N$, can be considered, in the most general case, a function of a set of variables:

$$v = F\left(\sigma_y, K_{IC}, \Delta\sigma_{fl}, \Delta K_{th}, E, \Delta K, h, a_{in}, d; 1-R\right) \tag{11}$$

The application of Buckingham's Π Theorem [14] reduces the number of dependencies by introducing suitable dimensionless numbers:

$$\begin{aligned} v &= \left(\frac{K_{IC}}{\sigma_y}\right)^2 \Phi\left(\frac{\Delta\sigma_{fl}}{\sigma_y}, \frac{\Delta K_{th}}{K_{IC}}, \frac{E}{\sigma_y}, \frac{\Delta K}{K_{IC}}, \frac{\sigma_y^2}{K_{IC}^2}h, \frac{\Delta\sigma_{fl}^2}{\Delta K_{th}^2}a_{in},\right. \\ &\quad \left. \times \frac{\sigma_y^2}{K_{IC}^2}d; 1-R\right) \\ &= \left(\frac{K_{IC}}{\sigma_y}\right)^2 \Phi\left(\frac{\Delta\sigma_{fl}}{\sigma_y}, \frac{\Delta K_{th}}{K_{IC}}, \frac{E}{\sigma_y}, \frac{\Delta K}{K_{IC}}, \frac{h}{r_p}, \frac{a_{in}}{a_0}, \frac{d}{r_p}; 1-R\right) \end{aligned} \tag{12}$$

where the dimensionless numbers in parenthesis are called Π_i (i = 1..0.8). These numbers can be reduced further from eight by assuming incomplete similarity in the dimensionless numbers Π_4, Π_5, Π_6, Π_7 and Π_8. This leads to a power-law dependency on the various numbers which has been confirmed by experimental trends or theoretical arguments [13–15]. As a result of this assumption, a generalized representation of fatigue crack growth is derived:

$$v = \left(\frac{K_{IC}^{2-\beta_1}}{\sigma_y^2}\right)\Delta K^{\beta_1}\left(\frac{h}{r_p}\right)^{\beta_2}\left(\frac{a}{a_0}\right)^{\beta_3}\left(\frac{d}{r_p}\right)^{\beta_4}(1-R)^{\beta_5}\Phi^* \tag{13}$$

where Φ^* is a dimensionless function of the remaining dimensionless numbers. According to this approach, the experimentally observed deviations from the simplest Paris' power-law regime is the result of incomplete self-similarity in the various dimensionless numbers, a situation often occurring in the case of intermediate asymptotic behaviours. As a result, the following expressions for the generalized Paris' law parameters m^* and C^* are obtained:

$$\begin{aligned} m^* &= \beta_1 \\ C^* &= \left(\frac{K_{IC}^{2-m}}{\sigma_y^2}\right)\left(\frac{h}{r_p}\right)^{\beta_2}\left(\frac{a}{a_0}\right)^{\beta_3}\left(\frac{d}{r_p}\right)^{\beta_4}(1-R)^{\beta_5}\Phi^* \end{aligned} \tag{14}$$

This generalized mathematical representation encompasses several improved versions of the Paris' law proposed during the last few decades to interpret anomalous deviations from the simplest power-law regime suggested by Paris. For instance, the anomalous behaviour of short cracks has been interpreted in [16, 18] as a consequence of the fractal roughness of crack surfaces. Independently, Jones et al. [5] have proposed a different interpretation based on elasto-plastic effects (see [18] for a critical comparison of the various scaling laws). Grain-size effects on the Paris' and Wöhler's curves have been interpreted by invoking the incomplete self-similarity assumption in the dimensionless number d/r_p (see Eq. (14)), together with the grain-size dependency of the yield strength according to the Hall–Petch law [19].

The problem of size-scale effects has received much less attention so far. Examining the recent experimental results obtained by Luke et al. [8] and shown in Fig. 2, we note that size-scale effects lead to a vertical shift of the Paris' curve corresponding to different specimen sizes, with a slight change in its slope. This mathematically corresponds to $C^* \propto h^{\beta_2}$ with $\beta_2 > 0$.

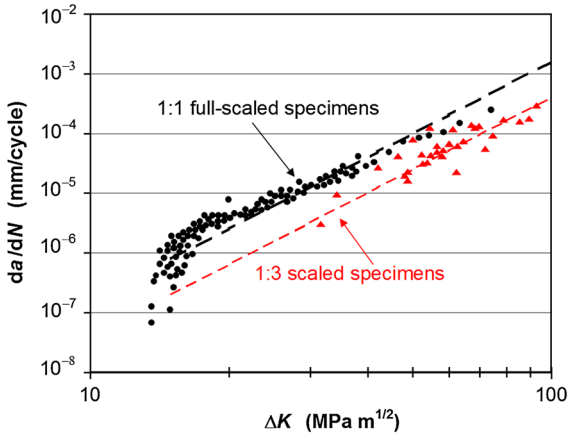

Fig. 5 The effect of the specimen size, h, on the Paris' curve (with incomplete self-similarity)

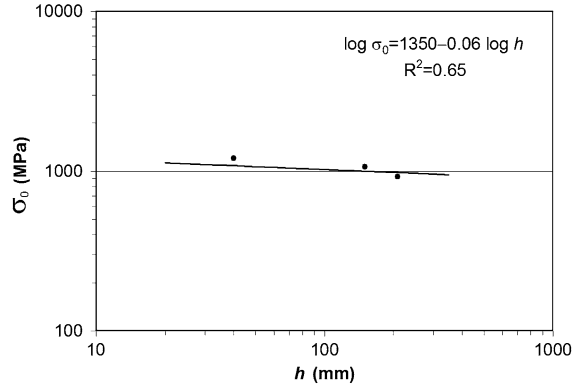

Fig. 6 The effect of the specimen size, h, on the coefficient σ_0 of the Wöhler's curve (with incomplete self-similarity)

To provide an experimental confirmation, we determine the parameters of the Paris' curve for the 1:3 down-scaled specimens in Fig. 2 by performing a best-fitting of the experimental data using a power-law equation. The result of this operation is shown in Fig. 5 (red triangles and dashed red line, please refer to the online version for colours). According to Eq. (14), the coefficient C^* of the Paris' curve of the 1:1 full-scaled specimens can be related to that of the 1:3 down-scaled specimens by the following relation:

$$C^*(1:1) = C^*(1:3)\left(\frac{h_{1:1}}{h_{1:3}}\right)^{\beta_2} = C^*(1:3) \times 3^{\beta_2} \tag{15}$$

where the scaling ratio $h_{1:1}/h_{1:3}$ is equal to 3 for the present case. Using this value of $C^*(1{:}1)$, a good agreement between theoretical predictions and experimental results is achieved with $\beta_2 = 1.25$, see the black dots and the dashed black line in Fig. 5.

Regarding the Wöhler's diagram, the situation is more complex, since Eq. (10) already predicts size-scale effects even without incomplete self-similarity. The experimental correct trend can be captured by introducing into Eq. (10) a size-scale dependent coefficient $C^* \propto h^{\beta_2}$ instead of a size-independent parameter C. As a result, the following scaling law for σ_0 is derived:

$$\sigma_0 = (\pi a_0)^{-1/2}(h/C^*)^{1/m} \propto \left(h/h^{\beta_2}\right)^{1/m} \propto h^{(1-\beta_2)/m} \tag{16}$$

To predict a shift of the Wöhler's curves to the left, as experimentally observed in Fig. 3, the intercept σ_0 has to be reduced by increasing the specimen size. Mathematically, this can be achieved if the scaling exponent $(1 - \beta_2)/m$ is negative valued, i.e., for $\beta_2 > 1$. To provide a confirmation, we estimate the intercepts σ_0 of the three curves in Fig. 3 corresponding to three different specimen sizes. This is done by extending these curves down to $N = 1$. The corresponding intercepts σ_0 are finally plotted versus the specimen size h in Fig. 6. The slope of the best-fitting line in this bi-logarithmic diagram is $(1 - \beta_2)/m$. In spite of the large uncertainty associated to the few available data points (coefficient of regression $R^2 = 0.65$), we estimate $(1 - \beta_2)/m \cong -0.06$. Since $m = 4$ according to the slope of the Paris' curves in Fig. 5, we finally determine $\beta_2 \cong 1.25$ from the size-scale effects on the Wöhler's curves. It is very important to remark that the value of this exponent is in perfect agreement with that independently estimated from the size-scale effects on the Paris' curves [see Fig. 5 and the discussion related to the determination of β_2 entering Eq. (15)].

4 Crack-size effects on the Paris' and Wöhler's curves

In the case of notched specimens, as demonstrated in Sect. 2, the integration of Paris' law leads to a Wöhler's curve whose exponent n is equal to m. In reality, the slope $1/n$ is often smaller than $1/m$, about one-third or one forth. An attempt to interpret the transition from the Wöhler to the Paris regime has been proposed in [20] by using a theory based on

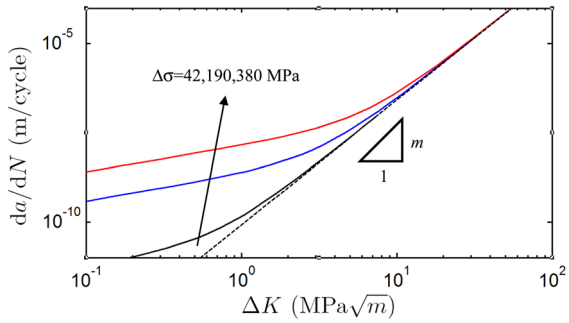

Fig. 7 The effect of the crack size on the Paris' curve ($a_0 = 92$ μm)

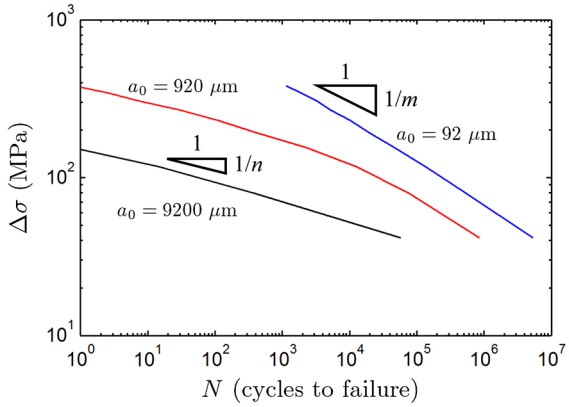

Fig. 8 The effect of the crack size on the Wöhler's curve

quantized fracture mechanics and an asymptotic matching approach. These main findings show that the tail of the Paris' curve near the fatigue threshold deviates from the Paris' power-law regime and depends on the applied stress range. Notably, the higher the stress range, the higher the crack growth rate for a given stress-intensity factor range. In the Wöhler's diagram, on the other hand, they found a transition from the Basquin power-law of the type (1b) to a power-law with an exponent $1/m$ typical of the integration of the Paris' curve by increasing the initial crack size. According to that model, specimens with physically long cracks should have a shorter life than specimens with short cracks. This trend, obtained as a direct consequence of asymptotic matching, seems to be in contradiction with the fact that short cracks have a faster crack growth rate than long cracks in the Paris' plot.

To resolve this inconsistency between the two trends, we propose the use of the fractal model of crack growth proposed in Paggi and Carpinteri [16] for describing the crack growth of short cracks. As a direct consequence of incomplete self-similarity in the dimensionless number a/a_0, the crack growth equation is:

$$\frac{da}{dN} = C\left(1+\frac{a_0}{a}\right)^{\frac{1}{2}\left(1+\frac{m}{2}\right)} \Delta K^m, \tag{17}$$

where a_0 is the characteristic length of short cracks, also called El Haddad crack length, for more details refer to Paggi and Carpinteri [16]. We propose now the application of Eq. (17) to the same material analyzed in Pugno et al. [20], i.e., the SAE1045 steel. To obtain the Wöhler's curve from Eq. (17), a numerical integration is performed, a procedure not done in previous publications.

The effect of the crack size on the Paris' curve is shown in Fig. 7 for different applied stress ranges, $a_0 = 92$ μm, $m = 3.5$ and $C = 8.2 \times 10^{-13}$. By increasing the applied stress range, the deviation from the Paris' power-law regime (shown with a dashed line in Fig. 7) for short cracks is quite remarkable.

The numerical integration of the Paris curves for different stress ranges shown in Fig. 7 leads to one single Wöhler's curve. Repeating this computation for different values of a_0, we obtain the results depicted in Fig. 8. For an intrinsic very small crack length a_0, an initial defect is propagating rapidly since it belongs to the long crack regime and the resulting Wöhler's curve has a slope $1/m$. Its fatigue life is in general quite long, since the crack growth rate predicted by Paris' power-law is smaller than for short cracks. On the other hand, if the intrinsic crack size is much larger, most of the lifetime of the initial defect is spent in the short crack regime. In this case, the deviation from the power-law trend in Fig. 7 leads to a higher crack growth rate as compared to a physically long crack and the cycles to failure for a given applied stress range are lower than in the case of long cracks. Very interestingly, the slope of the Wöhler's curve is no longer $1/m$, but it is considerably reduced. In the present case, we find $n = 10.5$, with a reduction of about 1/3 with respect to $1/m$ and in reasonable good agreement with experimental data ($n = 11.1$).

5 Conclusion

In this article, the fundamental equations describing the phenomenon of fatigue in terms of crack growth

rate and cycles to failure have been determined. This equation set alone suggests that the Paris' curve is size-scale independent and that the Wöhler's curve depends on the initial crack size and on the specimen size. To capture the experimental trends, the hypothesis of incomplete self-similarity is put forward, following preceding studies carried out by the present authors. As a result of this assumption, which leads to a size-scale dependent coefficient C of the Paris' law, the correct scaling of the Paris' curves can be predicted.

As a confirmation of the incomplete self-similarity assumption, it is proven that, up to a certain degree of accuracy related to the few available experimental data, the size-scale dependency of the coefficient C deduced from the Paris' diagram is able to explain the scaling of the Wöhler's curves as well. As a general trend, size-scale effects on the Paris' curves are more pronounced than on the Wöhler's curves. By increasing the specimen size, the crack growth rate increases and the fatigue life decreases. Due to the non-conservativeness of these trends, modifications to the existing material qualification standards are envisaged and additional experimental tests are considered to be essential to provide further confirmation for a wider range of materials. The incomplete self-similarity in the crack size is also quite relevant from the engineering point of view. In this work, in addition to the deviation from the Paris' law regime in the case of short cracks, the implication for the Wöhler's curves is explained. The transition from the short to the long crack regime leads to a modification in the slope of the curves and their shift in the Wöhler's diagram.

Acknowledgments The support of the Italian Ministry of Education, University and Research to the Project FIRB 2010 Future in Research "Structural mechanics models for renewable energy applications" (RBFR107AKG) is gratefully acknowledged.

References

1. Lazzeri, L., Salvetti, A., 1996. An experimental evaluation of fatigue crack growth prediction models. Proc. 1996 ASIP Conference, Vol. I, 477–508
2. Paris, P.C., 1962. The growth of cracks due to variations in load. Doctoral Dissertation, Lehigh University, Lehigh
3. Paris PC, Erdogan F (1963) A critical analysis of crack propagation laws. ASME J Basic Eng 85D:528–534
4. Paris PC, Gomez MP, Anderson WP (1961) A rational analytic theory of fatigue. Trend Eng 13:9–14
5. Jones R, Molent L, Pitt S (2008) Similitude and the Paris crack growth law. Int J Fatigue 30:1873–1880
6. Weibull W (1951) A statistical distribution function of wide applicability. ASME J Appl Mech A6:293–297
7. Beretta S, Zerbst U (2011) Damage tolerance of railway axles. Eng Fract Mech 78:713–862
8. Luke M, Varfolomeev I, Lütkepohl K, Esderts A (2011) Fatigue crack growth in railway axles: assessment concept and validation tests. Engng Fract Mech 78:714–730
9. Makino T, Kato T, Hirakawa K (2011) Review of the fatigue damage tolerance of high-speed railway axles in Japan. Engng Fract Mech 78:810–825
10. Barenblatt GI, Botvina LR (1980) Incomplete self-similarity of fatigue in the linear range of fatigue crack growth. Fatigue Fract Eng Mater Struct 3:193–202
11. Barenblatt GI (1980) Scaling, self-similarity and intermediate asymptotics. Cambridge University Press, Cambridge, p 1996
12. Ritchie RO (2005) Incomplete self-similarity and fatigue-crack growth. Int J Fract 132:197–203
13. Ciavarella M, Paggi M, Carpinteri A (2008) One, no one, and one hundred thousand crack propagation laws: a generalized Barenblatt and Botvina dimensional analysis approach to fatigue crack growth. J Mech Phys Solids 56:3416–3432
14. Carpinteri A, Paggi M (2009) A unified interpretation of the power laws in fatigue and the analytical correlations between cyclic properties of engineering materials. Int J Fatigue 31:1524–1531
15. Carpinteri A, Paggi M (2011) Dimensional analysis and fractal modelling of fatigue crack growth. J ASTM Int 8:1–13
16. Paggi M, Carpinteri A (2009) Fractal and multifractal approaches for the analysis of crack-size dependent scaling laws in fatigue. Chaos, Solitons Fractals 40:1136–1145
17. Wöhler, A., 1860. Versuche über die Festigkeit Eisenbahnwagenachsen. Z. Bauwesen 10
18. Carpinteri A, Paggi M (2010) A unified fractal approach for the interpretation of the anomalous scaling laws in fatigue and comparison with existing models. Int J Fract 161:41–52
19. Plekhov O, Paggi M, Naimark O, Carpinteri A (2011) A dimensional analysis interpretation to grain size and loading frequency dependencies of the Paris and Wöhler curves. Int J Fatigue 33:477–483
20. Pugno N, Ciavarella M, Cornetti P, Carpinteri A (2006) A generalized Paris' law for fatigue crack growth. J Mech Phys Solids 54:1333–1349